Monitoring complex formation in the blood-coagulation cascade using aptamer-coated SAW sensors

T.M.A. Gronewold, S. Glass, E. Quandt, M. Famulok*

Center of Advanced European Studies and Research, Aptamer Biosensors, Ludwig-Erhard-Allee 2, 53175 Bonn, Germany

Abstract

Specific binding of the anticoagulants heparin and antithrombin III to the blood clotting cascade factor human thrombin was recorded as a function of time with a Love-wave biosensor array consisting of five sensor elements. Two of the sensor elements were used as references. Three sensor elements were coated with RNA or DNA aptamers for specific binding of human thrombin. The affinity between the aptamers and thrombin, measured using the biosensor, was within the same range as the value of K_D measured by filter binding experiments. Consecutive binding of the thrombin inhibitors heparin, antithrombin III or the heparin–antithrombin III complex to the immobilized thrombin molecules, and binding of a ternary complex of heparin, anithrombin III, and thrombin to aptamers was evaluated. The experiments showed attenuation of binding to thrombin due to heparin–antithrombin III complex formation. Binding of heparin activated the formation of the inhibitory complex of antithrombin III with thrombin about 2.7-fold. Binding of the DNA aptamer to exosite II appeared to inhibit heparin binding to exosite I.
© 2004 Elsevier B.V. All rights reserved.

Keywords: Thrombin; Inhibitors; Aptamer; Biosensor; SAW

1. Introduction

A prototype Love-wave sensor with a detection limit of approximately 75 pg/cm² for proteins reversibly bound to a reusable aptamer surface was previously described (Schlensog et al., 2004). To probe the applicability of this sensor system for the detection of protein–protein interactions, and to evaluate its potential as an array-based screening system, we expanded the Love-wave sensor to thrombin-binding DNA- and RNA-aptamers and sought to detect and quantify complex-formation with a variety of components of the blood-coagulation cascade.

Aptamers are nucleic acid-based receptor molecules that are isolated from combinatorial libraries of synthetic oligonucleotides by in vitro selection, an iterative process of adsorption, recovery and amplification of oligonucleotides that selectively bind to a protein target (Ellington and Szostak, 1990; Robertson and Joyce, 1990; Tuerk and Gold, 1990). The isolated oligonucleotides, RNAs, single-stranded DNAs, or chemically modified oligonucleotides, have the ability to recognize and bind nearly every class of ligand molecules with high affinity and specificity. In addition, aptamers can be readily adapted in a straightforward fashion in vitro to fulfill criteria such as stability, detectability, specificity, affinity, and small size, required for their broad application in research, diagnostics and therapy.

There is currently a large interest in developing protein chip array technologies. In most cases, specificity and affinity are added to the arrays by antibodies or antibody fragments, enzymes, or other selective binders. Attempts have been made to fabricate aptamer sensors, e.g. using an aptamer with immunoglobulin E as a ligand combined with a quartz crystal microbalance (Liss et al., 2002), and companies like SomaLogic (Boulder, CO, USA) are developing array systems that rely on small oligonucleotides or aptamers in which thymidine is replaced by a brominated deoxyuridine

---

* Corresponding author. Present address: Kekulé Institut für Organische Chemie und Biochemie, Gerhard-Domagk-Strasse 1, 53121 Bonn, Germany. Tel.: +49 228 731787; fax: +49 228 735388.

E-mail address: m.famulok@uni-bonn.de (M. Famulok).

so that proteins are irreversibly crosslinked to the surface and stained via their free amines (Ito, 2004).

Here we describe a Love-wave sensor (Schlensog et al., 2004) modified with either an RNA- or DNA-aptamer surface for the detection of human α-thrombin and porcine thrombin (White et al., 2001). To further monitor interactions of aptamer-immobilized thrombin with thrombin-binding proteins, we added the thrombin-specific inhibitors antithrombin III and heparin to the sensor. In a first approach, the human serine protease α-thrombin was specifically bound to an RNA-aptamer (White et al., 2001), immobilized on a SAM surface. Thrombin (factor IIa) exhibits enzymatic properties and is the last protease in the clotting cascade, converting soluble fibrinogen to insoluble fibrin that forms the fibrin gel either of a physiological plug or a pathological thrombus (Holland et al., 2000). Thrombin also has hormone-like properties and plays a central role in thrombosis, haemostasis, blood-coagulation and anticoagulation cascades, and platelet activation. Thereby, thrombin is directly or indirectly involved in a number of cardiovascular diseases (Stubbs and Bode, 1993).

In a second approach, we investigated binding of the inhibitors heparin and antithrombin III to the immobilized thrombin. Antithrombotic drugs act as anticoagulants. Antithrombin III, a member of the *serpin* superfamily, is an endogenous inhibitor of thrombin. It forms a tight complex with thrombin. Heparin, a naturally occurring mucopolysaccharide activates antithrombin III by inducing conformational changes (Chuang et al., 2001; Olson and Chuang, 2002). It activates antithrombin III by inducing conformational changes. Binding of a defined pentasaccharide unit (A-domain), unique in the sulphated glycosaminoglucan heparin, potentiates serine protease inhibition. The T-domain of heparin electrostatically attracts thrombin. It slides along the heparin strand, until it docks to an antithrombin III subunit (Sinaÿ, 1999; Stubbs and Bode, 1994).

2. Materials and methods

2.1. Love-wave sensor setup and immobilization of aptamers as sensing layers

For preparation of the sensor, an AT cut quartz crystal was processed by photolithography as previously described (Schlensog et al., 2004). The obtained sensor chips of Love-wave sensor type with five sensor elements were placed into a readout system (S-sens analytics), and the detected signals were recorded in real time using a standard PC.

A self assembled monolayer of 11-mercapto undecanoic acid (Sigma) was formed on the gold shielding. Their carboxyl groups were activated using 50 mM *N*-hydroxysuccinimide (NHS) and 200 mM *N*-(3-dimethylaminopropyl)-*N*-ethylcarbodiimide (EDC). RNA aptamers with the sequence 5′-NH$_2$–(CH$_2$)$_3$–GGG AAC AAA GCU GAA GUA CUU ACC C-3′ (White et al., 2001), synthesized by Dharmacon Inc. (Lafayette, CO, USA), or
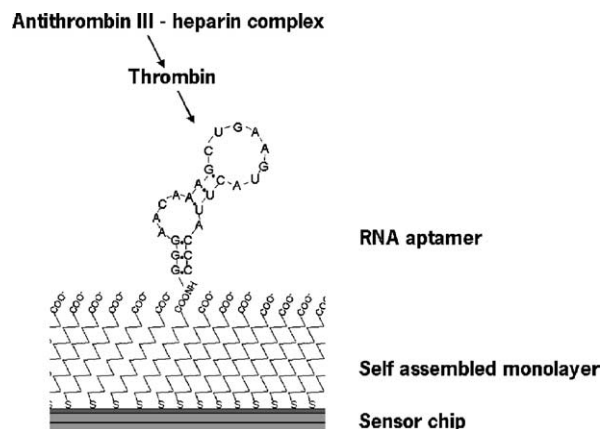

Fig. 1. RNA thrombin aptamer is coupled via carboxyl amide linkages to the Love-wave sensor surface covered with a 11-mercaptoundecanoic acid SAM. The aptamer specifically binds human α-thrombin. Thrombin forms a ternary complex with antithrombin III and heparin.

DNA aptamer with the sequence 5′-NH$_2$–(CH$_2$)$_3$–GGT TGG TGT GGT TGG (Bock et al., 1992), synthesized on an Expedite 8909 DNA Synthesizer (AME Bioscience), were coupled to the activated SAM via a 5′-amino linker (Schlensog et al., 2004) (Fig. 1).

2.2. Aptamer-analyte binding experiments

Binding experiments were performed at 23 °C in binding buffer (20 mM Tris–HCl, pH 7.4, 140 mM NaCl, 5 mM KCl, 1 mM MgCl$_2$). Human α-thrombin (HCT-0020), molecular weight 33,600 g/mol, and human antithrombin III (HCATIII-0120), molecular weight 58,000 g/mol, were purchased from Haematologic Technologies (Essex Junction, VT, USA). Elastase type I from porcine pancreas (E-1250), molecular weight 25,900 g/mol, and heparin from porcine intestinal mucosa (H5515) were obtained from Sigma. The heparin used was a crude solution with variable chain length of 45–50 residues and an average molecular weight of 12,000 g/mol. Heparin is physiologically active at a molecular weight above 6000 g/mol.

2.3. Calculation of mass loading

Displayed are the phase shifts measured with the Love-wave sensors. First, the difference of sensor and reference signal was evaluated. Bound masses were calculated using the sensitivity of the Love-wave sensor 419 [° cm^2/μg] (Schlensog et al., 2004) under the assumption that the value is generally applicable. Additional sensitivity values have been determined for proteins in the range from 2000–200,000 g/mol, showing variations of less than 8%. Concentrations were calculated with the molecular weights (2.2).

2.4. Control experiments

For filter binding experiments, 1 nM 3′-P^{32}-endlabelled RNA aptamer was incubated at 37 °C in 20 mM HEPES pH

7.4, 150 mM NaCl, 2 mM $CaCl_2$ with varying concentrations of thrombin ranging from 10 nM to 1.5 μM. This buffer led to the same binding results as the binding buffer. After 30 min. of incubation, the mixtures were applied to a 96-well Minifold® I Spot-/Dot-blot array equipped with a Protran 0.45 μm pore size nitrocellulose membrane (Schleicher & Schuell) and washed with binding buffer. Experiments were performed in triplets. The membrane-bound $3'$-P^{32}-RNA aptamers were quantified with a Fujifilm FLA-3000 phosphor imager.

Additional binding experiments were performed with a BIAcore 3000 system. The aptamers were coupled to the gold surface of BIAcore AU chips in flow-through, with similar surface preparation and conditions used as in the Love-wave sensor. Mass loading on the BIAcore chip was calculated assuming that a signal change of 1 response unit equals a mass loading of 1 pg/mm^2 (Jönsson et al., 1991).

3. Results

3.1. Interaction on a solid phase compared to solution

We performed titration experiments by nitrocellulose filter binding (Fig. 2A) to determine the solution K_D of the

thrombin/RNA aptamer complex. Unspecific binding to the membrane was corrected using a reference without protein. The fraction of aptamer was determined relative to the level of initially incubated aptamer and plotted against the initial protein concentration. A best curve fit was applied under the assumption that only one molecule of thrombin protein was bound per RNA aptamer molecule. The fitted K_D value of the RNA aptamer for thrombin determined in solution was about 294 ± 30 nM. It has been shown that the amount of RNA aptamer bound to thrombin varies to some extent with the manufacturer and quality of both the protein and the aptamer (data not shown). Fig. 2 shows solution/solid phase titration curves generated by chip-based Love-wave sensor (Fig. 2D) and BIAcore 3000 sensor (Fig. 2B). The displayed real-time sensor curves of the Love-wave sensor (Fig. 2C) display the difference phase signal of a sensor element covered with the immobilized RNA aptamer and a reference element. Each starts at baseline when injected while running buffer. Injections of different concentrations of thrombin start at $t_i = 100$ s. Thrombin concentration reaches its maximum within the first 30 s. During the injection period, the analyte/ligand complex reaches the equilibrium value at the given concentration of the binding partners. The total volume of the sample loop was 200 μl. The flow rate was 40 μl/min so that the estimated duration of an injection is $\Delta t = 300$ s. Towards the end
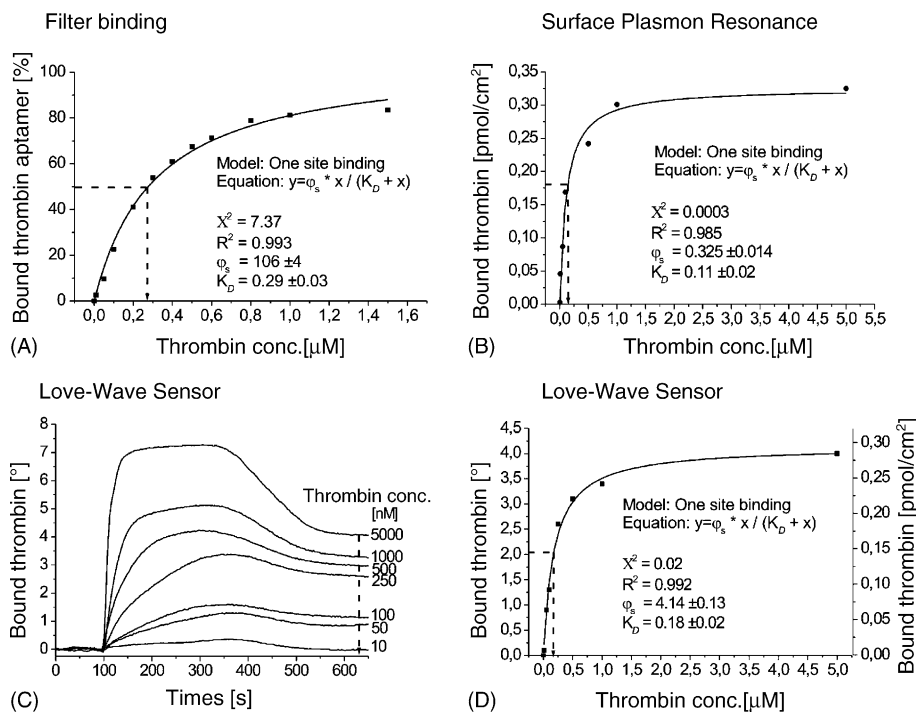

Fig. 2. Binding of thrombin to RNA aptamer. χ^2 = standard deviation; R^2 = correlation coefficient; φ_s = saturation, maximal binding of aptamers or surface with aptamers at concentration $\rightarrow \infty$; K_D = dissociation constant. (A) Filter binding test: displayed are filter binding results corrected for unspecific binding to the nitrocellulose membrane. The aptamer binds to thrombin with a fitted K_D value of ~294 nM. (B) BIAcore 3000: an RNA aptamer surface was generated with 7.0 pmol/cm^2. Concentrations of thrombin bound to RNA aptamer were evaluated. Displayed is the difference of sensor and reference signal plotted against the initial thrombin concentrations. The RNA aptamer binds thrombin with a fitted K_D-value of ~113 nM. (C) Love-wave sensor: comparison of binding curves of thrombin, concentrations as indicated, to an RNA aptamer surface regenerated with 0.1N NaOH. Displayed is the difference of sensor and reference signal. (D) Love-wave sensor: values of (A) as indicated by a dashed line in the diagram are plotted against the initial thrombin concentration. A best fit line was applied. The aptamer binds thrombin with a fitted K_D-value of ~181 nM.

of each injection interval, the concentration of thrombin in the sample loop decreases slightly due to dispersion with the following running buffer. Thus, the exact time until thrombin is completely exchanged for running buffer is not clearly defined. From glycerol injections can be estimated that the concentration of the analyte decreases within a time span of 100 s (data not shown). The phase shifts for Fig. 2D were derived at $t_i = 620$ s (dashed line). At this time, only running buffer is present over the sensing surfaces, and the difference phase follows the slow dissociation of bound thrombin from the surface.

We observed some unspecific interaction of the analyte with the surface. Both antithrombin III and thrombin are delivered as 120–220 μM solutions in 50% glycerol. During the flow of analyte-solutions over the surface, residual glycerol in the diluted analyte samples caused some of the phase shifts due to viscosity–density changes (McHale, 2003). Furthermore, the protein solutions appeared to exert electric influences to the Love-wave sensor to some extent during the injection of the analyte samples. After injection, running buffer is flowed over the sensor. At that point, the sensor signal results only from the analyte bound to the surface, without influences due to viscosity–density of the analyte solution. After completion of the measurement, the sensor-bound analyte is released at increased pH that unfolds the three-dimensional structure of the aptamer, and the baseline is reached again. To eliminate unspecific interactions from the signal and for the reasons described above, equilibrium values were plotted for both the BIAcore 3000 sensor (Fig. 2B) and the Love-wave sensor (Fig. 2D), and a best fit line was applied using the one site binding model. The RNA aptamer coupled to the surface yields a fitted K_D value for thrombin of about 113 ± 20 nM with the BIAcore 3000 sensor (Fig. 2B) and 181 ± 20 nM with the Love-wave sensor (Fig. 2D).

Both the correlation coefficient and the fitted K_D value were highest for the filter binding experiment (0.993 and 294 nM) followed by the Love-wave sensor (0.922 and 181 nM) and the BIAcore 3000 sensor (0.985 and 113 nM). In solution-phase, contact times were longer, while concentration of analytes declined due to binding. In both solution/solid-phase flow-through systems, equilibrium is reached with short contact times and a continuous flow of reagents of constant concentration across the sensor surface, resulting in lower K_D values. Those values are in the same range, considering the different methods used. For the DNA aptamer and its ligand thrombin, K_D values around 100–200 nM were determined with filter binding experiments (Bock et al., 1992; Schultze et al., 1994; Macaya et al., 1993; Tasset et al., 1997), 300 nM with a fiber-optic microarray (Lee and Walt, 2000), 450 nM with affinity chromatography (German et al., 1998), 50 nM with an optical sensor using fluorescence anisotropy (Potyrailo et al., 1998). This strongly suggests that the aptamers linked to the surface are fully functional with respect to thrombin-binding. They can be regenerated several times without loss of functionality (Schlensog et al., 2004).

Based on this set of experiments, we conclude that both the chosen aptamer density and the length of the $5'–NH_2–(CH_2)_3$-linker allow the ligand RNA aptamer to interact with its analyte thrombin protein nearly as well as in solution.

3.2. Detection of the ternary thrombin–antithrombin III–heparin complex

Further experiments were performed to monitor the formation of a complex of antithrombin III and heparin with thrombin bound to the RNA aptamer on the sensor. The following figures show the results of a series of injections in one single experiment on the same sensor chip, recorded over 28,000 s. Subsequent binding of 5 μM elastase, 5 μM thrombin, 5000 U/ml heparin, and 0.3 μM human antithrombin III were investigated by direct injections and by injections of preincubated complexes. Elastase was used to eliminate nonspecific binding. Thrombin and elastase both belong to the same family of serine proteases; thus, elastase was used in these experiments as a negative control and to quantify nonspecific binding to the RNA aptamer surface. The RNA aptamer surface was regenerated using 0.1N NaOH. For clarity, the graph was divided into separately shown binding curves consisting of binding events that belong together. The results of this set of experiments were repeated at least three times and verified by independent binding experiments using different detection systems such as the Love-wave sensor and the BIAcore surface plasmon resonance sensor (data not shown).

In the first set of experiments shown in Fig. 3A, the series of injections started with elastase. Thrombin was injected twice to ensure saturation of RNA aptamer sites. A mixture of the inhibitors heparin and antithrombin III was injected to evaluate binding to the bound thrombin. Concentrations used were optimized in preliminary experiments (data not shown). The surface was regenerated to yield baseline-level response of the sensor using 0.1N NaOH. In a second set of experiments, a mixture of thrombin, heparin, and antithrombin III was injected, followed by thrombin. Again, the surface was regenerated to baseline-levels with 0.1N NaOH.

From the equilibrium phase shifts, concentration and amount of each bound analyte were calculated (2.3) (Table 1A). Injection of elastase showed a phase shift of $0.15 \pm 0.02°$, corresponding to a concentration of about 14 ± 2 fmol/cm². The cognate analyte thrombin added 138 ± 13 fmol/cm² ($1.9 \pm 0.18°$) due to specific binding to its ligand. The second injection of thrombin added 33 ± 2 fmol/cm² ($0.46 \pm 0.03°$) to a total of 171 fmol/cm² thrombin. The value of 127 ± 15 fmol/cm² ($3.7 \pm 0.42°$) due to the subsequent injection of preincubated heparin–antithrombin III can be attributed to complexation of heparin–antithrombin III with 74% of the bound thrombin. After regeneration of the surface and injection of elastase with 32 ± 1 fmol/cm² ($0.35 \pm 0.03°$), 194 ± 7 fmol/cm²

Table 1
Summary of phase shifts detected

	Substance	Δ Phase shift [°]	Bound mass [ng/cm²]	Concentration [fmol/cm²]
(A) RNA aptamer				
1	Elastase	0.15 ± 0.02	0.36 ± 0.05	14 ± 2
2	Thrombin	1.9 ± 0.18	4.63 ± 0.43	138 ± 13
3	Thrombin	0.46 ± 0.03	1.06 ± 0.08	33 ± 2
4	Heparin–antithrombin III	3.7 ± 0.42	8.87 ± 1.02	127 ± 15
5	Regeneration			
6	Elastase	0.35 ± 0.03	0.84 ± 0.07	32 ± 1
7	Thrombin–heparin–antithrombin III	8.4 ± 0.32	20.04 ± 0.76	194 ± 7
8	Thrombin	1.0 ± 0.14	2.39 ± 0.34	71 ± 10
9	Regeneration			
10	Elastase	0.4 ± 0.05	0.72 ± 0.12	28 ± 5
11	Thrombin	2.6 ± 0.27	6.31 ± 0.64	188 ± 19
12	Antithrombin III	1.2 ± 0.11	2.98 ± 0.27	51 ± 5
13	Regeneration			
14	Elastase	0.3 ± 0.07	0.72 ± 0.17	28 ± 7
15	Thrombin	2.6 ± 0.26	6.19 ± 0.61	184 ± 18
16	Thrombin	0.6 ± 0.08	1.40 ± 0.19	42 ± 6
17	Heparin	~ 0	0	0
18	Regeneration			
19	Elastase	0.4 ± 0.07	0.95 ± 0.17	37 ± 7
20	Heparin	~ 0	0	0
21	Thrombin	3.2 ± 0.14	7.64 ± 0.34	227 ± 10
22	Regeneration			
23	Elastase	0.3 ± 0.08	0.72 ± 0.19	28 ± 7
24	Heparin–antithrombin III	-0.3 ± 0.05	-0.80 ± 0.12	-11 ± 2
25	Thrombin	3.4 ± 0.21	8.11 ± 0.51	242 ± 15
26	Regeneration			
(B) DNA aptamer				
1	Elastase	$0.18 \pm 0,06$	0.42 ± 0.13	16 ± 5
2	Thrombin	1.5 ± 0.17	3.58 ± 0.4	106 ± 12
3	Heparin–antithrombin III	0.31 ± 0.13	0.75 ± 0.31	11 ± 4
4	Regeneration			
5	Elastase	0.31 ± 0.09	0.75 ± 0.21	29 ± 8
6	Thrombin–heparin–antithrombin III	2.5 ± 0.71	6 ± 1.71	58 ± 16
7	Thrombin	2.3 ± 0.37	5.5 ± 0.88	163 ± 26
8	Regeneration			

Displayed are the difference of sensor and reference signal. Bound masses were calculated according to 2.3. (A) RNA aptamer and (B) DNA aptamer.

of the large ternary complex consisting of thrombin, heparin, and antithrombin III was bound ($8.4 \pm 0.32°$). The subsequent injection of the much smaller thrombin added only 71 ± 10 fmol/cm² ($1.0 \pm 0.14°$).

The binding of thrombin to the sensor-immobilized aptamer is specific. The first injection of thrombin to the aptamer-coated sensor led to a considerably higher response than the second injection, indicating that the aptamer-coated surface was almost saturated after the first injection. Therefore, the phase shift during and after injection of the mixture of heparin and antithrombin III can be attributed to specific binding of these ligands to the bound thrombin. Thus, this set of experiments indicates that the sensor detects the binding of antithrombin III and heparin to the aptamer/thrombin complex. In the second set we showed that the ternary complex of thrombin, antithrombin III, and heparin formed in solution binds to the RNA aptamer with coverage of a considerably large fraction of the surface.

3.3. Binding of antithrombin III and binding of heparin

The first two sets from Section 3.2 were followed by a third and fourth set of experiments on the same sensor chip after regeneration of the phase to baseline level (Fig. 3B). This showed the amount by which antithrombin III and heparin bind to thrombin. Elastase was injected firstly. Injections of thrombin were followed by injection of antithrombin III in the third set and heparin in the fourth set. From the equilibrium phase shifts, concentrations and amounts of each bound analyte were calculated (2.3) (Table 1A). Elastase injection resulted in a detection level corresponding to an amount of 28 ± 5 fmol/cm² ($0.4 \pm 0.05°$) bound on the sensor. Injection of thrombin added 188 ± 19 fmol/cm² ($2.6 \pm 0.27°$), and subsequent injection of antithrombin III 51 ± 5 fmol/cm² ($1.2 \pm 0.11°$), resulted in a coverage of about 27% of the thrombin bound on the aptamer surface. In the fourth set of measurements, elastase injection resulted in a detection level corresponding to an amount of
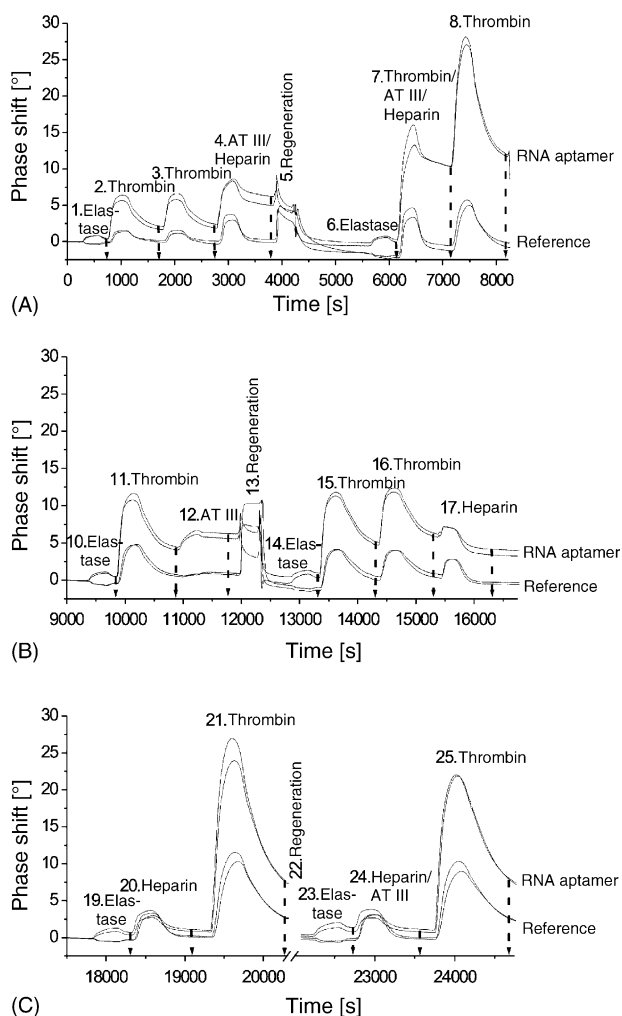
Fig. 3. Sequential binding of proteins to RNA aptamer. Displayed is the difference of sensor and reference signal. From the equilibrium phase shifts as indicated by dashed lines in the diagram, concentration and amount of each bound analyte were calculated. (A) Injections: 1. 5.0 μM elastase; (2) 5.0 μM thrombin; (3) 5.0 μM thrombin; (4) 5000 U/ml heparin incubated with 0.3 μM human antithrombin III; (5) 0.1N NaOH (regeneration); (6) 5.0 μM elastase; (7) 5 μM thrombin incubated with 5000 U/ml heparin and 0.3 μM human Antithrombin III; (8) 5.0 μM Thrombin. (B) Binding of antithrombin III and heparin to immobilized thrombin. Injections: (10) 5 μM elastase; (11) 5 μM thrombin; (12) 0.3 μM human antithrombin III; (13) 0.1N NaOH (regeneration); (14) 5 μM elastase; (15) 5 μM thrombin; (16) 5 μM thrombin; (17) 5000 U/ml heparin. (C) Unspecific binding of antithrombin III and heparin. Injections: (19) 5 μM elastase; (20) 5000 U/ml heparin; (21) 5 μM thrombin; (22) 0.1 N NaOH (regeneration); (23) 5 μM elastase; (24) 5000 U/ml heparin incubated with 0.3 μM human antithrombin III (25) 5 μM thrombin.

28 ± 7 fmol/cm^2 ($0.3 \pm 0.07°$), followed by thrombin binding of 226 ± 24 fmol/cm^2 ($3.2 \pm 0.34°$). Heparin showed almost the same binding to the reference and to the RNA aptamer surface.

The additional binding experiments with the single inhibitors were performed to estimate the factor by which heparin potentiates antithrombin III inhibition. Heparin shows no binding to thrombin without antithrombin III. Antithrombin III binds to a much lesser extent than the

heparin–antithrombin III complex. From this result it can be deduced that heparin potentiates total antithrombin III binding to thrombin by about 2.7 fold. The inhibition of thrombin by antithrombin III is a two-step process in which an initial, reversible complex is converted to a stable antithrombin III–thrombin complex in a first-order reaction. Heparin increases the affinity of the initial complex by nearly three orders of magnitude (Sheehan and Sadler, 1994). According to Myles et al. (1998) were k_{on}—values of the heparin–antithrombin III complex reduced two to fourfold in exosite I mutants, showing that heparin binds to exosite I of the thrombin protein when attached to antithrombin III. Antithrombin III itself has no major interaction with exosite I regardless of whether heparin is present or not.

3.4. Reverse sequence heparin–antithrombin III ahead of thrombin

The four sets from Sections 3.2 and 3.3 were followed by a fifth and sixth set of experiments on the same sensor chip to investigate, whether the phase shifts of heparin and antithrombin III were caused by non-specific interaction with the sensor surface, binding by the RNA aptamer, or whether the signal resulted from specific binding to immobilized thrombin protein (Fig. 3C). In both sets, elastase was injected firstly, and injections of thrombin were preceded by injection of one of the inhibitors; in the fifth set antithrombin III; and in the sixth set a mixture of antithrombin III and heparin. From the equilibrium phase shifts, concentration and amount of each bound analyte were calculated (2.3) (Table 1A). In the fifth set of experiments, elastase injection resulted in a detection level corresponding to an amount of 37 ± 7 fmol/cm^2 ($0.4 \pm 0.07°$), followed by an injection of heparin, where the difference of the phase shifts between sensor and reference elements was slightly negative. The injection of thrombin added 227 ± 10 fmol/cm^2 ($3.2 \pm 0.14°$).

In the sixth set of experiments elastase injection resulted in a detection level corresponding to an amount of 28 ± 7 fmol/cm^2 ($0.3 \pm 0.08°$), followed by the heparin–antithrombin III complex again with a slightly negative difference of phase shifts, and thrombin with 242 ± 15 fmol/cm^2 ($3.4 \pm 0.21°$). A negative difference of phase shifts corresponds to a higher binding to the reference element without the RNA aptamer. Thus, neither heparin nor the heparin–antithrombin III complex specifically interacted with the RNA aptamer surface, and the subsequent binding of thrombin was not inhibited.

3.5. Monitoring of complex formation with the DNA aptamer

To give further proof of the sensor, we replaced the RNA aptamer surface with a surface modified with the thrombin-binding DNA aptamer (Bock et al., 1992). In a previous study (Schlensog et al., 2004), the Love-wave sensor was combined with a DNA aptamer-based sensor surface for specific binding
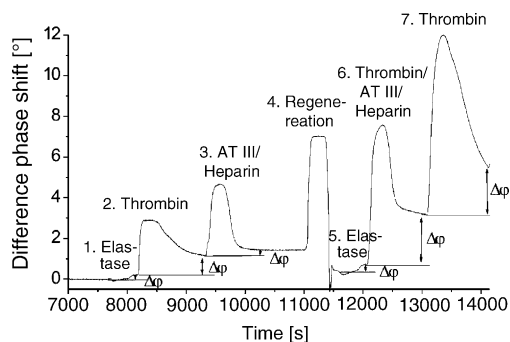
Fig. 4. Sequential binding of proteins to DNA aptamer. Displayed is the difference of sensor and reference signal. Injections: (1) 5.0 μM elastase; (2) 5.0 μM thrombin; (3) 5000 U/ml heparin incubated with 0.3 μM human antithrombin III; (4) 0.1N NaOH (regeneration); (5) 5.0 μM elastase; (6) 5 μM thrombin incubated with 5000 U/ml heparin and 0.3 μM human antithrombin III; (7) 5.0 μM thrombin. From the equilibrium phase shifts as indicated by arrows in the diagram, concentration and amount of each bound analyte were calculated.

of thrombin and iterative regeneration of the sensor to the same sensitivity. The fitted K_D-value determined in solution with repeated filter binding tests was about 300–400 nM. The DNA-aptamers linked to the surface of the Love-wave sensor and the BIAcore sensor yielded K_D-values in the same range. In this study we used the Love-wave sensor to analyze the complex formation of DNA aptamer-bound thrombin with the inhibitors antithrombin III and heparin (Fig. 4). After elastase, thrombin and the antithrombin III–heparin complex were injected. Baseline levels were reconstituted by washing with 0.1N NaOH, followed by injection of elastase, and a mixture of thrombin, antithrombin III and heparin. From the equilibrium phase shifts, concentrations and amount of each bound analyte were calculated (Table 1B). Elastase was bound at a density of 16 ± 5 fmol/cm^2 ($0.18 \pm 0.06°$). To this elastase-saturated surface, thrombin bound at a density of about 106 ± 12 fmol/cm^2 ($1.5 \pm 0.17°$). Injection of the antithrombin III–heparin complex added 11 ± 4 fmol/cm^2 ($0.31 \pm 0.13°$), equalling complexation with about 10% of the DNA aptamer-bound thrombin.

The surface was regenerated to baseline level and elastase injection resulted in a detection level corresponding to an amount of 29 ± 8 fmol/cm^2 ($0.31 \pm 0.09°$). Subsequent injection of the ternary thrombin–heparin–antithrombin III complex resulted in binding of 58 ± 16 fmol/cm^2 ($2.5 \pm 0.71°$). The injected thrombin added 163 ± 26 fmol/cm^2 ($2.3 \pm 0.37°$). Thus, after injection of the ternary complex, enough aptamers remained unbound so that about the same amount of thrombin was bound as to the free surface.

4. Discussion

4.1. Comparison of binding sites of anti-thrombin aptamers

We modified a Love-wave sensor device for detection of thrombin and thrombin inhibitors. Evidence was provided

that immobilization of RNA aptamers does not affect their ability to bind their cognate analytes. The RNA aptamer experiments showed that thrombin is bound to an amount of about 200 fmol/cm^2. Elastase, used as a negative control, was bound to 30 fmol/cm^2 or about 15% of the thrombin. In the experiments shown, thrombin was bound to the immobilized DNA aptamers to about 110 fmol/cm^2 or roughly half the amount of the RNA aptamer. Elastase was bound to about 16–30 fmol/cm^2 or about 15%. Differences may be attributed to the standardized evaluation of the curves at a specific time after injection so that eventually a stable value was not yet achieved. Solutions were injected consecutively in defined intervals during the complete experiment. Preliminary experiments using filter binding, the BIAcore 3000 sensor, or gel shift showed that the approximately 15% of residual binding to the DNA aptamer can be attributed to aptamer features; already minor differences in the small phase shifts observed result in relatively large variations (Schlensog et al., 2004, data not shown).

In binding studies using the RNA aptamer sensor, roughly three of four thrombin molecules bound to the RNA aptamer surface formed a complex with the much larger antithrombin III–heparin complex. The single inhibitory molecules did either not bind (heparin) or to only 27% (antithrombin III) of the immobilized thrombin and also did not bind unspecifically to the RNA aptamer surface. But heparin potentiated antithrombin III binding by a factor of 2.7. Coverage highly depended on surface density of the thrombin molecule, due to the size difference. Furthermore the proportion of bound ternary thrombin–heparin–antithrombin III complex to the following thrombin was about 194: 71 [fmol/cm^2], or roughly 3:1 for the RNA aptamer surface. It can be concluded that, on the thrombin protein molecule, the binding sites for the RNA aptamer and for the inhibitory heparin–antithrombin III complex are different and do not interfere with each other. Comparative experiments with the Love-wave sensor and a BIAcore 3000 sensor showed that antithrombin III binding highly depends on the accessibility of thrombin. High density of the smaller thrombin molecule resulted in lesser binding of antithrombin III (data not shown). Thus, the advantage of this sensor surface is the possibility to perform control experiments on the same surface after regeneration.

The data resulting from the experiments with the DNA aptamer sensor show that only about one in ten of the DNA aptamer-bound thrombin molecules formed a complex with antithrombin III–heparin, and the proportion of binding of the ternary thrombin–antithrombin III–heparin complex preceding thrombin was only 58: 163 [fmol/cm^2], or roughly 1: 3 for the DNA aptamer surface. By comparison, a relatively high amount of thrombin still was bound to the ternary complex-covered DNA aptamer surface. Taken together, these data suggest that the antithrombin III–heparin complex and the DNA aptamer reduce, but do not exclude, each others' binding properties.
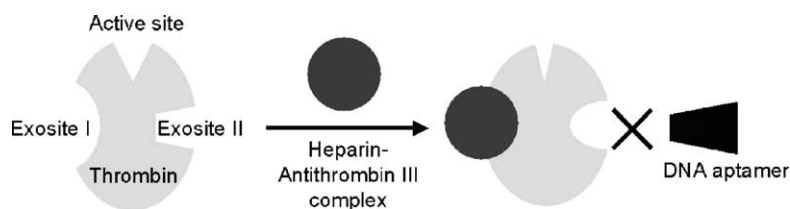
Fig. 5. Schematic representation of thrombin molecule undergoing a conformational change. Exosites I and II and the active site are not interfering with each other. According to the model induces binding to one of the exosites induces a conformational change in the thrombin molecule, thus modifying the distant second exosite.

4.2. Effect of the DNA aptamer on thrombin exosites I and II

For both inhibitors as well as for the DNA aptamer the binding sites on the thrombin molecule are well known. The thrombin molecule displays two positively charged exosites distant from the active site. Those exosites are thought to play a key role in determining the substrate specificity of thrombin. The results with the DNA aptamer were firstly the little complex formation of antithrombin III–heparin with the immobilized thrombin, and secondly the high amount of binding of thrombin after the ternary thrombin–antithrombin III–heparin complex was injected. Taken together, these results suggest that binding of the DNA aptamer to exosite II affects binding of the heparin–antithrombin III complex to exosite I. Two models explaining these effects are discussed in the following, the first one an interaction of the DNA aptamer with exosite I, and the second one an allosteric linkage of exosite II and exosite I. According to several lines of evidence, the DNA aptamer only binds to the anion binding exosite II (Paborsky et al., 1993; Tsiang et al., 1995; Bock et al., 1992; Padmanabhan et al., 1993). Holland et al. (2000) concluded from the effect of DNA aptamer on serpin-catalyzed thrombin inhibition reactions that the aptamer had virtually no influence on thrombin inhibition by antithrombin III with or without heparin binding to exosite I. Additionally, the binding sites for the DNA aptamer, exosite II, and for heparin, exosite I, are too distant for direct interaction. But extreme allosteric linkage has been reported between exosite I and exosite II of thrombin so that simultaneous occupation of both exosites is prevented (Fredenburgh et al., 1997; Liaw et al., 1998; Liu et al., 1991). The serpin mechanism involves dramatic conformational change in both the inhibitor and the inhibited protein (Huntington, 2003). It was observed that heparin induces an allosteric effect, causing dissociation of a complex consisting of thrombin and heparin cofactor II (Han and Tollefsen, 1998). According to this model induces binding of the DNA aptamer to exosite II a conformational change that prevents binding of heparin–antithrombin III to exosite I. Such a conformational change would explain our results. Formation of the ternary complex consisting of thrombin, heparin and antithrombin III could similarly prevent binding of the DNA aptamer to the thrombin molecule (Fig. 5). Our sensor cannot show these conformational changes, but we can measure the extent by which binding of one partner is reduced by binding of the second partner.

5. Conclusion

It can be deduced that the sensor may become a useful tool in proteomics and pharmacology for the determination of protein–protein interactions, and for the detection and verification of binding partners. Since the chosen methods allow coupling of various bio-molecules, a very versatile biosensor has been attained making interaction studies possible that allow binding sites to be distinguished on different analytes. It has been shown that the Love-wave sensor is a good and reliable device for following ligand/analyte interactions in real time. Efficient binding is reproducible, with low non-specific binding, and the sensor surfaces allow good regeneration in order to repeat the cycle of measurements. Another potential application of this biosensor lies in the screening of drugs or investigating the effects of macromolecular therapeutics on immobilized analytes. In particular, it might be possible to adapt this biosensor to the requirements of high throughput screening. New designs are currently being developed, e.g. other array formats, or in the fluidics, thus further improving the utility of the sensor.

References

Bock, L.C., Griffin, L.C., Latham, J.A., Vermaas, E.H., Toole, J.J., 1992. Selection of single-stranded DNA molecules that bind and inhibit human thrombin. Nature 355, 564–566.

Chuang, Y.-J., Swanson, R., Raja, S.M., Olson, S.T., 2001. Heparin enhances the specificity of antithrombin for thrombin and factor Xa independent of the reactive center loop sequence. Evidence for an exosite determinant of factor Xa specificity in heparin-activated antithrombin. J. Biol. Chem. 276 (18), 14961–14971.

Ellington, A.D., Szostak, J.W., 1990. In vitro selection of RNA molecules that bind specific ligands. Nature 346, 818–822.

Fredenburgh, J.C., Stafford, A.R., Weitz, J.I., 1997. Conformational changes in thrombin when complexed by serpins. J. Biol. Chem. 272, 25493–25499.

German, I., Buchanan, D.D., Kennedy, R.T., 1998. Aptamers as ligands in affinity probe capillary electrophoresis. Anal. Chem. 79, 4540–4545.

Han, J.-H., Tollefsen, D.M., 1998. Ligand binding to thrombin exosite II induces dissociation of the thrombin–heparin cofactor II (L444R) complex. Biochemistry 37, 3203–3209.

Holland, C.A., Henry, A.T., Whinna, H.C., Church, F.C., 2000. Effect of oligodeoxynucleotide thrombin aptamer on thrombin inhibition by heparin cofactor II and antithrombin. FEBS Lett. 484, 87–91.

Huntington, J.A., 2003. Mechanisms of glycosaminoglycan activation of the serpins in hemostasis. J. Thrombosis Haemostasis. 1 (7), 1535–1549.

Ito, Y., 2004. Design and synthesis of functional polymers by in vitro selection. Polym. Adv. Technol. 15 (1–2), 3–14.

Jönsson, U., Fägerstam, L., Ivarsson, B., Johnsson, B., Karlsson, R., Lundh, K., Löfås, S., Persson, B., Roos, H., Rönnberg, I., Sjölander, S., Stenberg, E., Ståhlberg, R., Urbaniszky, C., Östlin, H., Malmqvist, M., 1991. Real-time biospecific interaction analysis using surface plasmon resonance and a sensor chip technology. BioTechniques 11 (5), 620–627.

Lee, M., Walt, D.R., 2000. A fiber-optic microarray biosensor using aptamers as receptors. Anal. Biochem. 282, 142–146.

Liaw, P.C.Y., Fredenburgh, J.C., Stafford, A.R., Tulinsky, A., Austin, R.C., Weitz, J.I., 1998. Localization of the thrombin-binding domain on prothrombin fragment 2. J. Biol. Chem. 273 (15), 8932–8939.

Liss, M., Petersen, B., Wolf, H., Prohaska, E., 2002. An aptamer-based quartz crystal protein biosensor. Anal. Chem. 74 (17), 4488–4495.

Liu, L.-W., Ye, J., Johnson, A.E., Esmon, C.T., 1991. Proteolytic formation of either of the two prothrombin activation intermediates results in formation of a hirugen-binding site. J. Biol. Chem. 266 (35), 23632–23636.

Macaya, R.F., Schultze, P., Smith, F.W., Roe, J.A., Feigon, J., 1993. Thrombin-binding DNA aptamer forms a unimolecular quadruplex structure in solution. Proc. Natl. Acad. Sci. USA 90, 3745–3749.

McHale, G., 2003. Generalized concept of shear horizontal acoustic plate mode and Love wave sensors. Meas. Sci. Technol. 14, 1847–1853.

Myles, T., Church, F.C., Whinna, H.C., Monard, D., Stone, S.R., 1998. Role of thrombin anion-binding exosite-I in the formation of thrombin-serpin complexes. J. Biol. Chem. 273 (47), 31203–31208.

Olson, S.T., Chuang, Y.-J., 2002. Heparin activates antithrombin anticoagulant function by generating new interaction sites (exosites) for blood clotting proteinases. Trends Cardiovasc. Med. 12 (8), 331–338.

Paborsky, L.R., McCurdy, S.N., Griffin, L.C., Toole, J.J., Leung, L.L.K., 1993. The single stranded DNA aptamer-binding site of human thrombin. J. Biol. Chem. 268 (28), 20808–20811.

Padmanabhan, K., Padmanabhan, K.P., Ferrara, J.D., Sadler, J.E., Tulinsky, A., 1993. The structure of α-thrombin inhibited by a 15-mer single-stranded DNA aptamer. J. Biol. Chem. 268 (24), 17651–17654.

Potyrailo, R.A., Conrad, R.C., Ellington, A.D., Hieftje, G.M., 1998. Adapting selected nucleic acid ligands (aptamers) to biosensors. Anal. Chem. 70, 3407–3412.

Robertson, D.L., Joyce, G.F., 1990. Selection in vitro of an RNA enzyme that specifically cleaves single-stranded DNA. Nature 344 (6265), 467–468.

Schlensog, M., 2004 Schlensog, M.D., Gronewold, T., Tewes, M., Famulok, M., Quandt, E., 2004. A Love-wave biosensor using nucleic acids as ligands. Sens. Actuators B 101, 308–315.

Schultze, P., Macaya, R.F., Feigon, J., 1994. Three-dimensional solution structure of the thrombin-binding DNA aptamer d(GGTTGGTGTGGTTGG). J. Mol. Biol. 235, 1532–1547.

Sheehan, J.P., Sadler, J.E., 1994. Molecular mapping of the heparin-binding exosite of thrombin. Proc. Natl. Acad. Sci. USA 91, 5518–5522.

Sinaÿ, P., 1999. Synthetic chemistry: sugars slide into heparin activity. Nature 398, 377–378.

Stubbs, M.T., Bode, W., 1993. A player of many parts: the spotlight falls on thrombin's structure. Thrombosis Res. 69, 1–58.

Stubbs, M.T., Bode, W., 1994. Coagulation factors and their inhibitors. Curr. Biol. 4, 823–832.

Tasset, D.M., Kubik, M.F., Steiner, W., 1997. Oligonucleotide inhibitors of human thrombin that bind distinct epitopes. J. Mol. Biol. 272, 688–698.

Tsiang, M., Jain, A.K., Dunn, K.E., Rojas, M.E., Leung, L.L.K., Gibbe, C.S., 1995. Functional mapping of the surface residues of human thrombin. J. Biol. Chem. 270 (25), 16854–16863.

Tuerk, C., Gold, L., 1990. Systematic evolution of ligands by exponential enrichment: RNA ligands to bacteriophage T4 DNA polymerase. Science 249, 505–510.

White, R., Rusconi, C., Scardino, E., Wolberg, A., Lawson, J., Hoffman, M., Sullenger, B., 2001. Generation of species cross-reactive aptamers using toggle "SELEX". Mol. Therapy. 4 (6), 567–573.